2011

Arabidopsis G-protein interactome reveals connections to cell wall carbohydrates and morphogenesis

Karsten Klopffleisch

Nguyen Phan

Kelsey Augustin

Robert S. Bayne

Katherine S. Booker

See next page for additional authors

Authors

Karsten Klopffleisch, Nguyen Phan, Kelsey Augustin, Robert S. Bayne, Katherine S. Booker, Jose R. Botella, Nicholas C. Carpita, Tyrell Carr, Jin-Gui Chen, Thomas Ryan Cooke, Arwen Frick-Cheng, Erin J. Friedman, Brandon Fulk, Michael G. Hahn, Kun Jiang, Lucia Jorda, Lydia Kruppe, Chenggang Liu, Justine Lorek, Maureen C. McCann, Antonio Molina, Etsuko N. Moriyama, M. Shahid Mukhtar, Yashwanti Mudgil, Sivakumar Pattathil, John Schwarz, Steven Seta, Matthew Tan, Ulrike Temp, Yuri Trusov, Daisuke Urano, Bastian Welter, Jing Yang, Ralph Panstruga, Joachim F. Uhrig, and Alan M. Jones

Molecular Systems Biology 7; Article number 532; doi:10.1038/msb.2011.66
Citation: ***Molecular Systems Biology*** **7:532**

www.molecularsystemsbiology.com

molecular systems biology

REPORT

Arabidopsis G-protein interactome reveals connections to cell wall carbohydrates and morphogenesis

Karsten Klopffleisch[1,15], Nguyen Phan[2,15], Kelsey Augustin[3], Robert S Bayne[2], Katherine S Booker[2], Jose R Botella[4], Nicholas C Carpita[5], Tyrell Carr[2], Jin-Gui Chen[6], Thomas Ryan Cooke[7], Arwen Frick-Cheng[2], Erin J Friedman[2], Brandon Fulk[8], Michael G Hahn[7,9], Kun Jiang[2], Lucia Jorda[10], Lydia Kruppe[1], Chenggang Liu[2], Justine Lorek[11], Maureen C McCann[5], Antonio Molina[10], Etsuko N Moriyama[8], M Shahid Mukhtar[2,16], Yashwanti Mudgil[2,17], Sivakumar Pattathil[7], John Schwarz[12], Steven Seta[2], Matthew Tan[2], Ulrike Temp[1], Yuri Trusov[4], Daisuke Urano[2], Bastian Welter[1], Jing Yang[2], Ralph Panstruga[11,13,*], Joachim F Uhrig[1,*] and Alan M Jones[2,14,*]

[1] Botanical Institute, University of Cologne, Cologne, Germany, [2] Department of Biology, University of North Carolina at Chapel Hill, Chapel Hill, NC, USA, [3] Department of Computer Technology and Information Systems, Wayne State College, Wayne, NE, USA, [4] School of Agriculture and Food Science, University of Queensland, Brisbane, Queensland, Australia, [5] Department of Botany and Plant Pathology and Bindley Bioscience Center, Purdue University, West Lafayette, IN, USA, [6] Oak Ridge National Laboratory, Biosciences Division, Oak Ridge, TN, USA, [7] Complex Carbohydrate Research Center, University of Georgia, Athens, GA, USA, [8] School of Biological Sciences and Center for Plant Science Innovation, University of Nebraska-Lincoln, Lincoln, NE, USA, [9] Department of Plant Biology, University of Georgia, Athens, GA, USA, [10] Centro de Biotecnología y Genomica de Plantas (UPM-INIA), Universidad Politécnica de Madrid, Madrid, Spain, [11] Max-Planck Institute for Plant Breeding Research, Cologne, Germany, [12] Department of Biostatistics, University of North Carolina at Chapel Hill, Chapel Hill, NC, USA, [13] Unit of Plant Molecular Cell Biology, Institute for Botany, RWTH Aachen University, Aachen, Germany and [14] Department of Pharmacology, University of North Carolina at Chapel Hill, Chapel Hill, NC, USA
[15] These authors contributed equally to this work
[16] Present address: Department of Biology, CH106, University of Alabama at Birmingham, Birmingham, AL 35294, USA
[17] Present address: Department of Botany, University of Delhi, Delhi, India
* Corresponding authors. R Panstruga, Institute for Biology I, Aachen University, D-52056 Aachen, Germany. Tel.: + 49 241 802 6655; Fax: + 49 241 802 2637; E-mail: panstruga@bio1.rwth-aachen.de or JF Uhrig, Botanical Institute, University of Cologne, D-50674 Cologne, Germany. Tel.: + 49 221 470 3902; Fax: + 49 221 470 5062; E-mail: Joachim.Uhrig@uni-koeln.de or AM Jones, Department of Biology, University of North Carolina at Chapel Hill, Coker Hall, CB#3280, Chapel Hill, NC 27599-3280, USA. Tel.: + 1 919 962 6932; Fax: + 1 919 962 1625; E-mail: alan_jones@unc.edu

Received 4.5.11; accepted 17.8.11

The heterotrimeric G-protein complex is minimally composed of Gα, Gβ, and Gγ subunits. In the classic scenario, the G-protein complex is the nexus in signaling from the plasma membrane, where the heterotrimeric G-protein associates with heptahelical G-protein-coupled receptors (GPCRs), to cytoplasmic target proteins called effectors. Although a number of effectors are known in metazoans and fungi, none of these are predicted to exist in their canonical forms in plants. To identify *ab initio* plant G-protein effectors and scaffold proteins, we screened a set of proteins from the G-protein complex using two-hybrid complementation in yeast. After deep and exhaustive interrogation, we detected 544 interactions between 434 proteins, of which 68 highly interconnected proteins form the core G-protein interactome. Within this core, over half of the interactions comprising two-thirds of the nodes were retested and validated as genuine *in planta*. Co-expression analysis in combination with phenotyping of loss-of-function mutations in a set of core interactome genes revealed a novel role for G-proteins in regulating cell wall modification.
Molecular Systems Biology **7**: 532; published online 27 September 2011; doi:10.1038/msb.2011.66
Subject Categories: plant biology; signal transduction
Keywords: AGB1; Arabidopsis; GPA1; heterotrimeric G-proteins; RGS1

Introduction

Heterotrimeric G-proteins couple a myriad of extracellular signals, including light, ions, peptides hormones, neurotransmitters, and protein ligands, to intracellular changes in ion flux, enzymatic activity, protein proximities, and trafficking. Classically, the G-protein heterotrimer is activated by cell-surface receptors (G-protein-coupled receptors, GPCRs) that trigger the Gα-subunit of the heterotrimer to release GDP, thus enabling the Gα-subunit to bind to GTP. GTP binding is accompanied by structural rearrangements that disengage the Gβγ interaction and result in heterotrimer dissociation (Sprang, 1997). The free subunits then relay signals by interacting with downstream proteins collectively called effectors, because they 'effect' the cellular changes mentioned above. G-protein signaling is terminated after the Gα-subunit hydrolyzes GTP to GDP and the heterotrimer re-associates. Gα proteins provide specificity between GPCRs and effectors, amplify signal

transduction, serve as a point of signal modulation, and act as timing devices that control signaling lifespan.

In metazoans, there are hundreds of GPCRs as well as dozens of effectors, modulators, and scaffold proteins that interact with the heterotrimer or its dissociated subunits (Temple *et al*, 2010). However, few, if any, of these are encoded in plant genomes sequenced to date (Jones and Assmann, 2004). Because our understanding of G-protein signaling in plants critically depends on knowing the constellation of proteins operating in this network and the relationship of each effector to each other, we chose an *ab initio* approach to assemble the G-protein interactome. Presumptive roles for G-protein signaling in several new pathways were revealed and one was pursued here.

Results and discussion

Generation of a high-quality G-protein interactome map using yeast two-hybrid screening

Aiming at the identification of regulators and effectors of heterotrimeric G-protein subunits in *Arabidopsis thaliana*, we performed comprehensive high-throughput yeast two-hybrid (Y2H) screening. Nine prey cDNA libraries made from diverse *Arabidopsis* tissues were screened 10 times using seven primary baits, including the subunits of the heterotrimeric G-proteins Gα (GPA1), Gβ/Gγ1 (AGB1/AGG1), Gβ/Gγ2 (AGB1/AGG2), (Ullah *et al*, 2001, 2003; Trusov *et al*, 2007), and regulator of G-protein signaling 1 (RGS1), Pirin (PRN), N-myc downregulated-like1 (NDL1), and receptor for activated C kinase1A (RACK1A; Chen *et al*, 2003, 2006; Lapik and Kaufman, 2003; Mudgil *et al*, 2009). To distinguish between potential effectors that interact with GPA1 in its active conformation only, and regulators interacting with GPA1 irrespective of its activation state, three variants of GPA1 were used as bait constructs: a constitutive active form (Q222L), the wild-type protein, and a mutant version with accelerated GTPase activity (G220A). Potential false positives were excluded both by re-cloning and retesting positive interactions, as well as excluding known common false positives (Methods and Supplementary Experimental Procedures). The complete data set is available in Supplementary Table 1, in Arabidopsis Protein Interaction Database (AtPID, ID:FDS1176001), and in a public database dedicated to Arabidopsis G-protein signaling (AGIdb), http://bioinfolab.unl.edu/AGIdb.

In accordance with published data, our screenings identified AGG1, AGG2, and NDL1 as interactors of AGB1, and thylakoid formation 1 (THF1) as an effector of the constitutive active form of GPA1 (Huang *et al*, 2006; Mudgil *et al*, 2009). From the total of 206 unique prey proteins from the first round of screenings, 14 secondary baits (ANNAT1, ARD1, CDC48B, NDL1, RACK1B, RACK1C, SYP23, TGA1, UNE16, VAP27, AT1G05000, AT1G52760, AT4G26410, and AT5G14240) were chosen, because these interacted with two or more of the primary baits. Interestingly, the interaction data reveal a highly interconnected network, with many proteins identified as interaction partners of two or more of the bait proteins. High local connectivity supports the close functional relationship of the proteins involved, and proteins sharing interaction partners have an increased probability of interacting themselves (Milo *et al*, 2002; Barabasi and Oltvai, 2004). Furthermore, interactions within three- and four-protein-interaction loop motifs are considered reliable and functionally meaningful (Spirin and Mirny, 2003; Wuchty *et al*, 2003; Yeger-Lotem *et al*, 2004). Therefore, we focused on the biconnected core (two-core) of the network composed of 69 proteins interacting with at least two other proteins in the network. Thirty-eight of these proteins were analyzed further by individually testing all possible pair-wise combinations for interaction in yeast. This approach led to the identification of 64 additional interactions, resulting in a highly interconnected core network (68 nodes, 167 edges) with an average node degree of 4.1 (Figure 1). A comparison of the gene ontology annotations of the core network to the genome indicated enrichment in these categories: plasma membrane, nucleus, cytosol, endoplasmic reticulum, ribosome, protein binding, nucleotide binding, structural molecule activity, responses to biotic/abiotic stresses, developmental processes and cell organization, and biogenesis (Supplementary Figure S1). Homologous interacting protein pairs from other organisms (interlogs) were not found.

In planta confirmation of protein–protein interactions

We randomly selected 41 central proteins from the core network and 8 outside the core to test 78 interactions *in planta* by bimolecular fluorescence complementation (BiFC). In addition, 28 negative controls comprising both soluble and membrane proteins were included. Seventy-four of the 78 tested protein pairs, but none of the negative control pairs, complemented yellow fluorescent protein (YFP) fluorescence, indicating *in planta* interaction, thereby corroborating the Y2H data. The test pairs were selected after passing stringent experimental and topological filters (Supplementary Experimental Procedures). Our validation rate is higher than expected given the previously observed detection overlap between Y2H and orthogonal validation assays (Braun *et al*, 2009). This is likely due to the applied filtering of validated interactions, although formally it cannot be excluded that use of a larger and more diverse set of random negative controls would detect a higher background and hence necessitate more stringent scoring. The majority of the BiFC signals were present in the cytoplasm and/or the cell periphery of epidermal pavement cells. Notably, some tested interactions seem to be restricted to the nucleus *in planta*, e.g., MYC2-ARD1, AGB1-MYB, and UNE16-MYB, while others preferentially take place in guard cells, e.g., RGS1-TGA1 and ARD1-EXGT-A1 (Supplementary Figure S2).

Correlation of gene expression supports the reliability of the G-protein interactome map

Correlated expression frequently is an indicator of co-functionality of genes in common pathways and processes (Persson *et al*, 2005; Hirai *et al*, 2007; Humphry *et al*, 2010), and interacting proteins, particularly proteins that are part of network motifs, are often significantly co-expressed (Bhardwaj and Lu, 2009). We therefore interrogated correlation of expression of

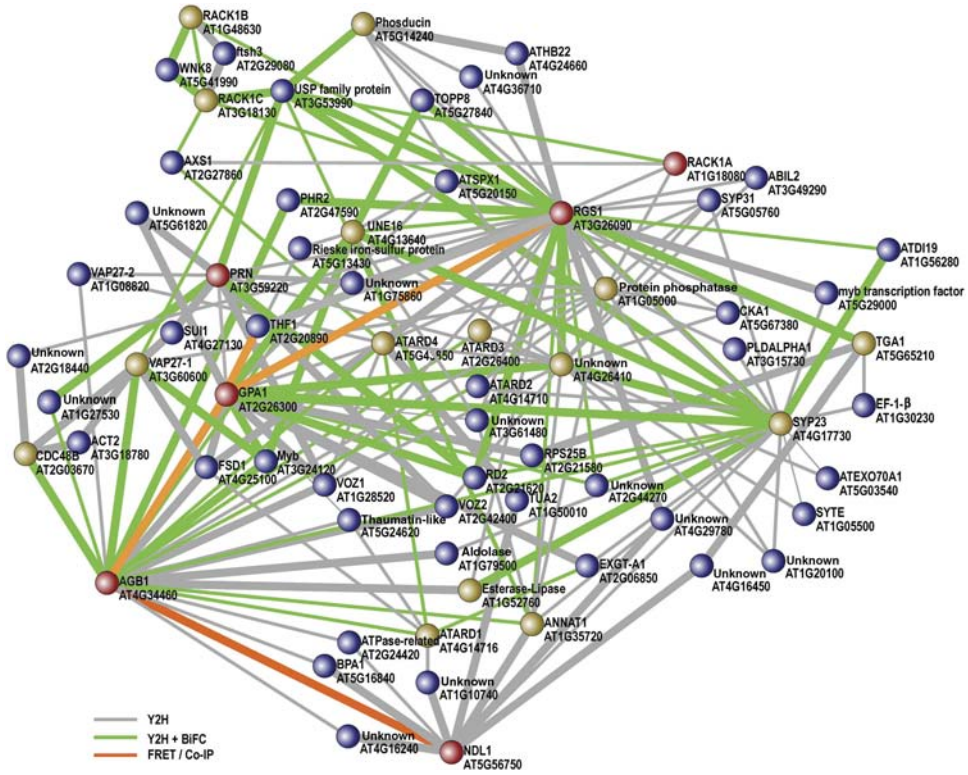

Figure 1 Arabidopsis heterotrimeric G-protein core interactome. Only those proteins from the interactome data set are shown that possess at least two connections within the network (two-core). Red nodes highlight published components of G-protein signaling in Arabidopsis that were used as primary baits in the Y2H screenings. Proteins used as baits for the second round of screens are shown in brown. Gray lines (edges) represent interactions detected with the Y2H system. Green edges represent interactions shown with both the Y2H system and BiFC. Orange edges represent interactions found in our Y2H screenings that were published and confirmed by FRET analyses or co-immunoprecipitation previously (Lapik and Kaufman, 2003; Adjobo-Hermans *et al*, 2006; Huang *et al*, 2006; Mudgil *et al*, 2009). The AGB1-ARD1 through ARD4 confirmations are as described in Friedman *et al* (2011). Thick edges indicate protein pairs with significantly correlated expression profiles (Supplementary Table S1).

the gene pairs derived from our interaction analyses. To establish a threshold of significance for this type of analysis, 69 gene pairs encoding proteins well documented to physically interact were analyzed ('gold standard', Supplementary Table S1). The thresholds were established using permutation testing to account for multiple testing practices. The expression profiles of the gold standard protein pairs were significantly correlated as compared with a random selection. We then calculated correlation of gene expression for 385 gene pairs from the G-protein interactome across the four GENEVESTIGATOR categories: Anatomy, Development, Mutation, and Stimulus. In total, 90, 15, 178, and 196 of the 385 tested pairs across the four respective categories showed a significant correlation of gene expression (Figure 1, Supplementary Table S1, and AGIdb, http://bioinfolab.unl.edu/AGIdb). Overall, the average expression correlation of the gene pairs was significantly higher than the reliability of the G-protein interaction network made up of the 69 previously documented gene pairs.

The core interactome points to a previously unknown role for G-proteins in cell wall composition

The interactome provided many new leads to test a role of G-proteins in Arabidopsis cell function, some of which are known while many are new. For example, manual inspection of the interactome revealed several potentially interesting interactions between the G-protein core and proteins that may either directly (e.g., enzymes) or indirectly (e.g., transcription factors) regulate cell wall composition or structure (Supplementary Table S1). Among the cell wall-associated enzymes in this group, the predominant candidates have known or predicted functions toward xylose biosynthesis or metabolism. Xylose is present in plant cell walls primarily in two polysaccharides, xyloglucan and xylan, both of which are found in Arabidopsis tissues. Therefore, we hypothesized that the cells lacking a functional G-protein complex would have an altered xyloglucan and/or xylan content or structure.

We first tested for alterations in cell wall composition across a selection of G-protein mutants using infrared microscopy, a rapid method to detect global changes in cell wall composition (McCann *et al*, 2007), followed by principal component (PC) analysis. Mutants tested included *agb1*, *gpa1*, *rgs1*, *suppressor of G-beta1* (*SGB1*), and a double mutant defective in both *GPA1* and *AGB1*. The *gpa1–3*, *rgs1–2*, and *sgb1–2* single mutants could not easily be discriminated from Col-0 wild type. However, the *agb1–2* mutant and the *gpa1–4 agb1–2* double mutant could be discriminated from Col-0 at 80% correct assignment using four PCs for the double mutant, and 78% using five PCs for the *agb1* single mutant (Supplementary

Figure S3A–D). The loading for PC2 indicates differences in cell wall ester, protein content, and some carbohydrate features between Col-0 and *agb1*.

As infrared microscopy does not allow unambiguous identification of the altered carbohydrates, we next analyzed wild-type and mutant cell walls for monosaccharide content via gas–liquid chromatography. Small but significant differences in the mole % of one of the major cell wall pentoses, xylose, were observed in both the *agb1* mutant and *gpa1 agb1* double mutant compared with wild type. While the *agb1* single mutant exhibited a slight but statistically significant decrease in xylose mole %, the *gpa1 agb1* double mutant showed a statistically significant increase in the proportion of cell wall xylose (Supplementary Table S1). The opposing phenotypes suggest that the action is primarily through GPA1, as loss of AGB1 would increase the activated pool and loss of GPA1 would decrease it (Ullah *et al*, 2003). Specific increases or decreases in xylose content alone suggest alterations in either xylan or xyloglucan structures.

To determine more precisely the identity of the polysaccharide affected by the mutations, and to gain a broader picture of cell wall changes in the mutant plants, cell walls of wild-type and mutant plants were quantitatively profiled for their glycan epitope content (glycome profiling). Glycome profiling involves enzyme-linked immunosorbent assay-based screening of sequential extracts of cell walls, using a set of ~150 cell wall glycan-directed monoclonal antibodies that resolve into 18 groups recognizing diverse epitopes present on most major classes of plant cell wall polysaccharides (Pattathil *et al*, 2010). Leaf and root tissues were isolated from *gpa1* and *agb1* single mutants, the *gpa1 agb1* double mutant, the *gpa1 agb1 agg1 agg2* quadruple mutant, and wild-type plants. The glycome profiles of leaf and root cell walls from mutants showed some differences when compared with each other and to the profiles from wild-type cell walls. The altered glycome profiles were particularly evident in the case of the leaf cell wall extracts of the mutants, where the binding patterns of the xylan-3 and xylan-4 groups of antibodies varied in all of the mutants (Figure 2A and Supplementary Table S1 and Supplementary Figure S3E). In the *gpa1 agb1* double mutant and *gpa1* single mutant, a reduced abundance of xylan-3 (P=7.2e−12 in the double mutant and P=1.8e−14 in the single mutant) and

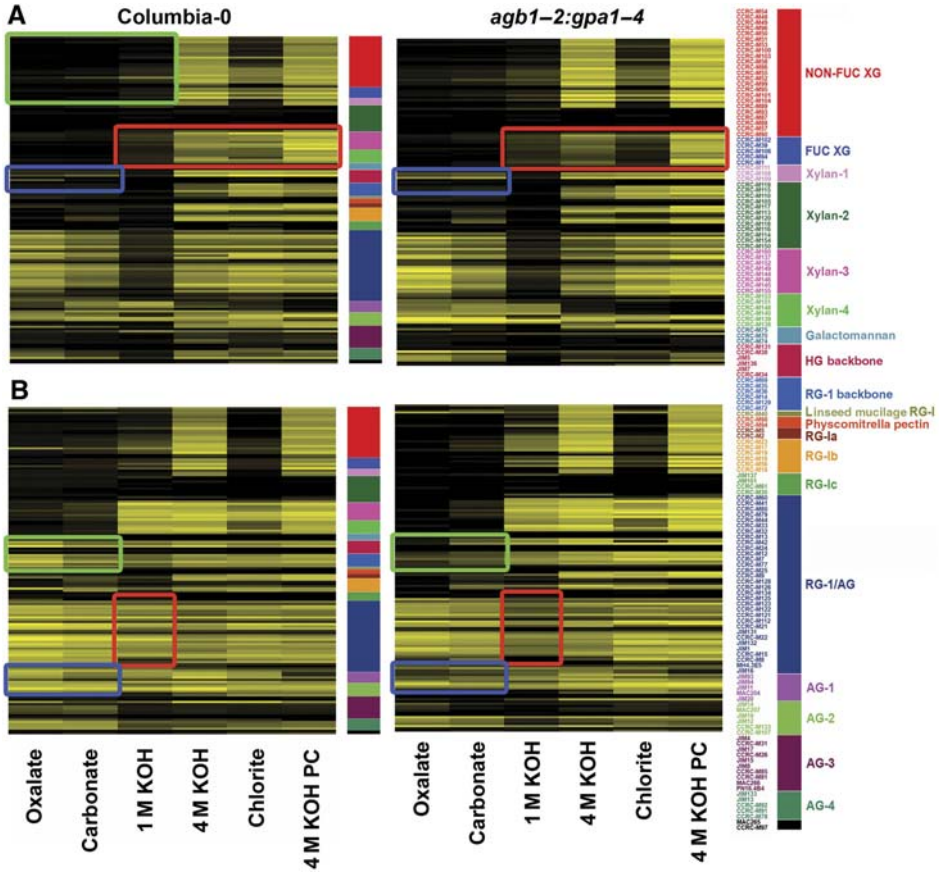

Figure 2 Glycome profiling of sequential cell wall extracts prepared from leaves (**A**) and roots (**B**) of the *agb1*, *gpa1* mutant and wild-type (Columbia-0, Col-0) plants. Heat maps of enzyme-linked immunosorbent assay (ELISA) data obtained by screening the sequential carbohydrate extracts with 150 glycan-directed monoclonal antibodies (Pattathil *et al*, 2010). The panel on the right lists the array of monoclonal antibodies used (left-hand side) and groups them according to the principal cell wall glycan (right-hand side) recognized by the antibodies (Pattathil *et al*, 2010). The reagents used for various extraction steps are identified at the bottom of each column in the heat map. The yellow-black scale indicates the strength of the ELISA signal: bright yellow depicts strongest binding and black indicates no binding. The colored outlines highlight the changes in the antibody binding patterns to the extracts of the mutants compared with WT. (A) The red box outlines the changes in the xylan-3 and xylan-4 antibodies, blue box outlines the changes in the pectic backbone antibodies, and green box outlines the changes in xyloglucan-directed antibodies. (B) Green box outlines the changes in the pectic backbone antibodies, red box outlines the changes in the RG-1/AG antibodies, and the blue box outlines the changes in the AG-1 and AG-2 antibodies. A full data set of the glycome profiles of all mutants can be found in Supplementary Figures S2 and S3.

xylan-4 (P=1.8e−5 in the double mutant and P=1.1e−5 in the single mutant) epitopes was observed in the chlorite fraction in comparison with the corresponding fraction from wild-type cell walls (Figure 2A). Analyses were carried out using ANOVA models on each antibody classification group (Supplementary Experimental Procedures), and the results are provided in Supplementary Table S1. Additionally, the chlorite fractions from the leaf cell walls of *gpa1* and *gpa1 agb1 agg1 agg2* quadruple mutants contained reduced levels of xylan-3 and xylan-4 epitopes. Subtle changes in the glycome profiles for some mutant cell walls were also noted in the binding patterns of antibodies against pectic backbone and xyloglucan-directed antibodies (Figure 2A and Supplementary Figure S3E). Overall, these results indicate that structural changes in the leaf cell walls of mutants were mostly related to the structural features of xylan or to the integration of xylan into the cell walls during its biosynthesis.

The mutants also showed differences in their root cell wall glycome profiles compared with that of wild-type plants, although the dissimilarities were in different groups of antibodies than those observed in the leaf glycome profiles. Invariably, in all mutants, there was a notable reduction in the levels of pectic backbone epitopes (homogalacturonan, rhamnogalacturonan I backbone epitopes) in the oxalate and carbonate extracts compared with the corresponding extracts from wild-type walls. There was also a subtle reduction in the release of pectic rhamnogalacturonan I/arabinogalactan (RG-I/AG) epitopes in the 1 M KOH fractions of the mutants. Additionally, altered binding patterns of the AG-1 and AG-2 groups of antibodies to the oxalate and carbonate fractions of mutants was observed (Figure 2B and Supplementary Figure S3F). These data suggest that the mutations in the genes studied here also affect root cell wall structure, primarily by altering the extractability of pectic polysaccharides.

In summary, the glycome profiles of the mutant wall extracts indicate that mutations in heterotrimeric G-protein complex components lead to alterations of the overall cell wall structure, thereby resulting in changes in the extractability of primarily xylan epitopes in leaf tissues and pectic backbone epitopes in root tissues.

Mutants of G-protein interactors share a stomatal density phenotype

Alterations in cell wall composition can confer anomalous morphological features and one quantifiable anomaly is the stomatal pattern of the epidermis (Chen *et al*, 2009; Guseman *et al*, 2010). Previous genetic analysis revealed that *GPA1* and *AGB1* antagonistically modulate stomatal density in Arabidopsis (Zhang *et al*, 2008). To assess whether any of the newly identified members of the G-protein interactome are co-involved in this process of aberrant morphogenesis, we quantified stomatal density at two different time points in seedlings of 17 plant lines carrying mutations in genes encoding proteins at nodes of the core interactome and compared them to Col-0 wild type. Our data confirmed the previously reported lower and higher stomatal density of *gpa1* and *agb1* single mutants, respectively, as well as the phenotype of the *gpa1 agb1* double mutant, which was reported to be intermediate between the *agb1* mutant and Col-0 wild type (Zhang *et al*, 2008). Five mutants showed either significantly ($P<0.1$) elevated or reduced stomatal density (Supplementary Table S1). These mutants relate to a diverse set of genes with yet unknown links to cell wall modification and/or morphogenesis.

Conclusions

We established a comprehensive protein–protein interaction network for Arabidopsis G-protein signaling pathway elements, greatly expanding our view of G-protein-coupled signaling. Interactome networks derived from high-throughput interactome projects have proven highly valuable for systems biology and the functional annotation of the genomes of a number of model organisms (Gavin *et al*, 2002; Li *et al*, 2004; Formstecher *et al*, 2005; Rual *et al*, 2005). An unbiased, partial, plant interactome data set (8000 by 8000 matrix) was published during review of the present work (Arabidopsis Interactome Mapping Consortium, 2011). In Arabidopsis, systematic protein interaction mapping projects focused on pre-selected groups of genes with specific structural or functional relation, such as particular transcription factor families, membrane proteins, virulence effectors, or proteins involved in cell cycle regulation (Zimmermann *et al*, 2004; de Folter *et al*, 2005; Lalonde *et al*, 2010; Van Leene *et al*, 2010; Mukhtar *et al*, 2011). Our focused interactome revealed G-protein interacting proteins with different subcellular localization and cell type specificity. A role for the G-protein interactome in cell wall biogenesis/metabolism was deduced from the predicted functions of identified interactors, the biochemical and immunological phenotype of G-protein mutants, and the morphological phenotype of mutants defective in G-protein interactors.

Materials and methods

Y2H methods

All bait constructs used in the primary and secondary screenings were tested for auto-activation, and the addition of 3-amino-1,2,4-triazole eliminated residual growth on selection media. To exclude potential screening artifacts ('technical false positives'; Finley, 2007; Venkatesan *et al*, 2009), *in vivo* recombination cloning of PCR products was used to re-clone the prey cDNAs in yeast, and interactions were pair wise reassessed with their respective baits as well as with negative controls. Only those prey clones that were positive with the bait and negative in the control experiment were taken into account. Preys representing known Y2H artifacts were discarded (Supplementary Experimental Procedures). Further details of the methods used for the interaction screens, including the nine cDNA libraries interrogated, are provided in Supplementary Experimental Procedures.

Arabidopsis G-Signaling Interactome Database

The protein interaction information that we obtained is publicly available through the Web-based database: *Arabidopsis* G-Signaling Interactome Database (AGIdb, http://bioinfolab.unl.edu/AGIdb). The AGIdb currently includes information from 544 unique protein pairs (currently 1058 interaction data obtained from different libraries and other experimental conditions) and allows users to access and search the entire data set. The interaction data can be downloaded in a table format that can be imported in Cytoscape (http://www.cytoscape.org/; Cline *et al*, 2007) and other network analysis software. Details of the specifications of the database are provided in Supplementary Experimental Procedures.

Genes that show correlated expression may share *cis*-acting elements in their promoters (5′ regulatory regions). Known *cis*-acting elements for each gene in the interactome were retrieved via a dedicated database (AtcisDB, http://arabidopsis.med.ohio-state.edu/AtcisDB/) and added to the interactome database. Comparative analysis revealed sets of shared *cis*-regulatory elements in case of some co-expressed interactome genes.

Bimolecular fluorescence complementation

BiFC was performed as described in Grigston *et al* (2008) with modifications as indicated in Supplementary Experimental Procedures. The higher extinction coefficient mediated by these second-generation BiFC vectors enabled analyses at lower expression levels, thus greatly lowering the false-positive rate. A positive-transformation control was included. Leaf samples were imaged using a Zeiss LSM710 confocal laser scanning microscope equipped with an Apochromat $\times 40$ (NA 1.2) water-immersion objective. The positive control for BiFC interaction used in each replicate was the AHP2 dimer (At3g29350). Twenty-eight negative control tests for core proteins against both membrane and soluble proteins were included (Supplementary Figure S1, panels 79–109).

Co-expression analyses

A detailed description of the methods used to determine the statistical significance of paired gene expression patterns is provided in the Supplementary Experimental Procedures material.

Cell wall analyses

Isolation of cell walls, FITR analysis, monosaccharide and linkage analyses, glycome profiling, and the statistical analyses used for glycome profiling are described in detail in the Supplementary Experimental Procedures material.

Supplementary information

Supplementary information is available at the *Molecular Systems Biology* website (www.nature.com/msb).

References

Adjobo-Hermans MJW, Goedhart J, Gadella Jr TWJ (2006) Plant G-protein heterotrimers require dual lipidation motifs of Gα and Gγ and do not dissociate upon activation. *J Cell Sci* **119:** 5087–5097

Arabidopsis Interactome Mapping Consortium (2011) Evidence for network evolution in an Arabidopsis interactome map. *Science* **333:** 601–607

Barabasi A-L, Oltvai ZN (2004) Network biology: understanding the cell's functional organization. *Nat Rev Genet* **5:** 101–113

Bhardwaj N, Lu H (2009) Co-expression among constituents of a motif in the protein-protein interaction network. *J Bioinform Comput Biol* **7:** 1–17

Braun P, Tasan M, Dreze M, Barrios-Rodiles M, Lemmens I, Yu H, Sahalie JM, Murray RR, Roncari L, de Smet A-S, Venkatesan K, Rual J-F, Vandenhaute J, Cusick ME, Pawson T, Hill DE, Tavernier J, Wrana JL, Roth FP, Vidal M (2009) An experimentally derived confidence score for binary protein-protein interactions. *Nat Meth* **6:** 91–97

Chen JG, Ullah H, Temple B, Liang J, Guo J, Alonso JM, Ecker JR, Jones AM (2006) RACK1 mediates multiple hormone responsiveness and developmental processes in Arabidopsis. *J Exp Bot* **57:** 2697–2708

Chen J-G, Willard FS, Huang J, Liang J, Chasse SA, Jones AM, Siderovski DP (2003) A seven-transmembrane RGS protein that modulates plant cell proliferation. *Science* **301:** 1728–1731

Acknowledgements

We are extremely grateful to Philip Zimmermann for allowing us to access the raw data in the GENEVESTIGATOR database. We thank Ms Abby Lin, Chapel Hill High School for lab assistance. This work was supported by the NSF 2010 Program (MCB-0723515) to AMJ, by the Deutsche Forschungsgemeinschaft to RP (DFG PA861/6-1) and JU (DFG UH119/6-1), by the US National Science Foundation Plant Genome Program (DBI-0923992) to MGH and by the Laboratory Directed Research and Development Program of Oak Ridge National Laboratory, managed by UT-Battelle, LLC, for the US Department of Energy under contract DE-AC05-00OR22725. The generation of the CCRC series of plant cell wall glycan-directed monoclonal antibodies used in this work was supported by the NSF Plant Genome Program (DBI-0421683).

Author contributions: Karsten Klopffleisch, Nicholas C Carpita, Jin-Gui Chen, and Nguyen Phan planned experiments, collected data, analyzed data, and wrote the manuscript. Kelsey Augustin and Brandon Fulk designed and created the database. Robert S Bayne, Tyrell Carr, Kun Jiang, and Erin J Friedman tested *in vivo* interactions. Katherine S Booker and Arwen Frick-Cheng performed phenotypic profiling. Jose R Botella managed project and shared unpublished data. Thomas Ryan Cooke, Lucia Jorda, Justine Lorek, Yashwanti Mudgil, Ulrike Temp, Yuri Trusov, Bastian Welter, and Lydia Kruppe collected data. Michael G Hahn planned experiments, collected data, analyzed data, wrote the manuscript, and funded the project. Chenggang Liu made many libraries. Maureen C McCann planned experiments, collected data, and analyzed data. Antonio Molina shared unpublished data. Etsuko N Moriyama planned and created the database. M Shahid Mukhtar made a library. Sivakumar Pattathil performed glycome profiling and analyzed data. John Schwarz designed and performed all statistical analyses and wrote the manuscript. Steven Seta performed genotyping. Matthew Tan assembled gene expression correlation data, analyzed, and wrote the manuscript. Daisuke Urano tested *in vivo* interactions and analyzed data. Jing Yang genotyped, collected data and managed *in vivo* testing. Ralph Panstruga and Joachim F Uhrig managed and funded the project, designed experiments, and wrote the manuscript. Alan M Jones managed and funded the project, designed experiments, collected data, analyzed data, and wrote the manuscript.

Conflict of interest

The authors declare that they have no conflict of interest.

Chen X-Y, Liu L, Lee E, Han X, Rim Y, Chu H, Kim S-W, Sack F, Kim J-Y (2009) The Arabidopsis callose synthase gene GSL8 is required for cytokinesis and cell patterning. *Plant Physiol* **150:** 105–113

Cline MS, Smoot M, Cerami E, Kuchinsky A, Landys N, Workman C, Christmas R, Avila-Campilo I, Creech M, Gross B, Hanspers K, Isserlin R, Kelley R, Killcoyne S, Lotia S, Maere S, Morris J, Ono K, Pavlovic V, Pico AR *et al* (2007) Integration of biological networks and gene expression data using Cytoscape. *Nat Protoc* **2:** 2366–2382

de Folter S, Immink RGH, Kieffer M, Parenicova L, Henz SR, Weigel D, Busscher M, Kooiker M, Colombo L, Kater MM, Davies B, Angenent GC (2005) Comprehensive interaction map of the Arabidopsis MADS box transcription factors. *Plant Cell* **17:** 1424–1433

Finley Jr RL (2007) *A Guide to Yeast Two-Hybrid Experiments*. Cambridge: Cell Press

Formstecher E, Aresta S, Collura V, Hamburger A, Meil A, Trehin A, Reverdy C, Betin V, Maire S, Brun C, Jacq B, Arpin M, Bellaiche Y, Bellusci S, Benaroch P, Bornens M, Chanet R, Chavrier P, Delattre O, Doye V *et al* (2005) Protein interaction mapping: a *Drosophila* case study. *Genome Res* **15:** 376–384

Friedman EJ, Wang HX, Perovic I, Deshpande A, Pochapsky TC, Temple BRS, Hicks SN, Harden TK, Jones AM (2011) ACI-REDUCTONE DIOXYGENASE 1 (ARD1) is an effector of the

heterotrimeric G protein β subunit in Arabidopsis. *J Biol Chem* **286:** 30107–30118

Gavin A-C, Bosche M, Krause R, Grandi P, Marzioch M, Bauer A, Schultz J, Rick JM, Michon A-M, Cruciat C-M, Remor M, Hofert C, Schelder M, Brajenovic M, Ruffner H, Merino A, Klein K, Hudak M, Dickson D, Rudi T *et al* (2002) Functional organization of the yeast proteome by systematic analysis of protein complexes. *Nature* **415:** 141–147

Grigston JC, Osuna D, Scheible WR, Stitt M, Jones AM (2008) D-glucose sensing by a plasma membrane regulator of G signaling protein, AtRGS1. *FEBS Lett* **582:** 3577–3584

Guseman JM, Lee JS, Bogenschutz NL, Peterson KM, Virata RE, Xie B, Kanaoka MM, Hong Z, Torii KU (2010) Dysregulation of cell-to-cell connectivity and stomatal patterning by loss-of-function mutation in Arabidopsis CHORUS (GLUCAN SYNTHASE-LIKE 8). *Development* **137:** 1731–1741

Hirai MY, Sugiyama K, Sawada Y, Tohge T, Obayashi T, Suzuki A, Araki R, Sakurai N, Suzuki H, Aoki K, Goda H, Nishizawa OI, Shibata D, Saito K (2007) Omics-based identification of Arabidopsis Myb transcription factors regulating aliphatic glucosinolate biosynthesis. *Proc Natl Acad Sci USA* **104:** 6478–6483

Huang J, Taylor JP, Chen J-G, Uhrig JF, Schnell DJ, Nakagawa T, Korth KL, Jones AM (2006) The plastid protein THYLAKOID FORMATION1 and the plasma membrane G-protein GPA1 interact in a novel sugar-signaling mechanism in Arabidopsis. *Plant Cell* **18:** 1226–1238

Humphry M, Bednarek P, Kemmerling B, Koh S, Stein M, Goebel U, Stueber K, Pislewska-Bednarek M, Loraine A, Schulze-Lefert P, Somerville S, Panstruga R (2010) A regulon conserved in monocot and dicot plants defines a functional module in antifungal plant immunity. *Proc Natl Acad Sci USA* **107:** 21896–21901

Jones AM, Assmann SM (2004) Plants: the latest model system for G-protein research. *EMBO Rep* **5:** 572–578

Lalonde S, Sero A, Pratelli R, Pilot G, Chen J, Sardi MI, Parsa SA, Kim D-Y, Acharya BR, Stein EV, Hu H-C, Villiers F, Takeda K, Yang Y, Han YS, Schwacke R, Chiang W, Kato N, Loqu D, Assmann SM *et al* (2010) A membrane protein/signaling protein interaction network for Arabidopsis version AMPv2. *Front Plant Physiol* **1:** 24

Lapik VR, Kaufman LS (2003) The Arabidopsis cupin domain protein AtPirin1 interacts with the G protein α subunit GPA1 and regulates seed germination and early seedling development. *Plant Cell* **15:** 1578–1590

Li S, Armstrong CM, Bertin N, Ge H, Milstein S, Boxem M, Vidalain P-O, Han J-DJ, Chesneau A, Hao T, Goldberg DS, Li N, Martinez M, Rual JF, Lamesch P, Xu L, Tewari M, Wong SL, Zhang LV, Berriz GF *et al* (2004) A map of the interactome network of the metazoan *C. elegans*. *Science* **303:** 540–543

McCann MC, Defernez M, Urbanowicz B, Tewari JC, Langewisch T, Olek A, Wells B, Wilson RH, Carpita NC (2007) Neural network analyses of infrared spectra for classifying cell wall architectures. *Plant Physiol* **143:** 1314–1326

Milo R, Shen-Orr S, Itzkovitz S, Kashtan N, Chklovskii D, Alon U (2002) Network motifs: simple building blocks of complex networks. *Science* **298:** 824–827

Mudgil Y, Uhrig JF, Zhou J, Temple B, Jiang K, Jones AM (2009) Arabidopsis N-MYC DOWNREGULATED-LIKE1, a positive regulator of auxin transport in a G protein-mediated pathway. *Plant Cell* **21:** 3591–3609

Mukhtar MS, Carvunis A-R, Dreze M, Epple P, Steinbrenner J, Moore J, Tasan M, Galli M, Hao T, Nishimura MT, Pevzner SJ, Donovan SE, Ghamsari L, Santhanam B, Romero V, Poulin MM, Gebreab F, Gutierrez BJ, Tam S, Monachello D *et al* (2011) Independently evolved virulence effectors converge onto hubs in a plant immune system network. *Science* **333:** 596–601

Pattathil S, Avci U, Baldwin D, Swennes AG, McGill JA, Popper Z, Bootten T, Albert A, Davis RH, Chennareddy C, Dong R, O'Shea B, Rossi R, Leoff C, Freshour G, Narra R, O'Neil M, York WS, Hahn MG (2010) A comprehensive toolkit of plant cell wall glycan-directed monoclonal antibodies. *Plant Physiol* **153:** 514–525

Persson S, Wei H, Milne J, Page GP, Somerville CR (2005) Identification of genes required for cellulose synthesis by regression analysis of public microarray data sets. *Proc Natl Acad Sci USA* **102:** 8633–8638

Rual J-F, Venkatesan K, Hao T, Hirozane-Kishikawa T, Dricot A, Li N, Berriz GF, Gibbons FD, Dreze M, Ayivi-Guedehoussou N, Klitgord N, Simon C, Boxem M, Milstein S, Rosenberg J, Goldberg DS, Zhang LV, Wong SL, Franklin G, Li S *et al* (2005) Towards a proteome-scale map of the human protein-protein interaction network. *Nature* **437:** 1173–1178

Spirin V, Mirny LA (2003) Protein complexes and functional modules in molecular networks. *Proc Natl Acad Sci USA* **100:** 12123–12128

Sprang SR (1997) G protein mechanisms: Insights from structural analysis. *Ann Rev Biochem* **66:** 639–678

Temple B, Jones C, Jones A (2010) Evolution of a signaling nexus constrained by protein interfaces and conformational states. *PLoS Comp Biol* **6:** e1000962

Trusov Y, Rookes JE, Tilbrook K, Chakravorty D, Mason MG, Anderson D, Chen J-G, Jones AM, Botella JR (2007) Heterotrimeric G protein γ subunits provide functional selectivity in Gβγ dimer signaling in Arabidopsis. *Plant Cell* **19:** 1235–1250

Ullah H, Chen J-G, Temple B, Boyes DC, Alonso JM, Davis KR, Ecker JR, Jones AM (2003) The β subunit of the Arabidopsis G protein negatively regulates auxin-induced cell division and affects multiple developmental processes. *Plant Cell* **15:** 393–409

Ullah H, Chen J-G, Young J, Im K-H, Sussman MR, Jones AM (2001) Modulation of cell proliferation by heterotrimeric G protein in *Arabidopsis*. *Science* **292:** 2066–2069

Van Leene J, Hollunder J, Eeckhout D, Persiau G, Van De Slijke E, Stals H, Van Isterdael G, Verkest A, Neirynck S, Buffel Y, De Bodt S, Maere S, Laukens K, Pharazyn A, Ferreira PCG, Eloy N, Renne C, Meyer C, Faure J-D, Steinbrenner J *et al* (2010) Targeted interactomics reveals a complex core cell cycle machinery in *Arabidopsis thaliana*. *Mol Syst Biol* **6:** 397

Venkatesan K, Rual J-F, Vazquez A, Stelzl U, Lemmens I, Hirozane-Kishikawa T, Hao T, Zenkner M, Xin X, Goh K-I, Yildirim MA, Simonis N, Heinzmann K, Gebreab F, Sahalie JM, Cevik S, Simon C, de Smet A-S, Dann E, Smolyar A *et al* (2009) An empirical framework for binary interactome mapping. *Nat Meth* **6:** 83–90

Wuchty S, Oltvai ZN, Barabasi AL (2003) Evolutionary conservation of motif constituents in the yeast protein interaction network. *Nat Genet* **35:** 176–179

Yeger-Lotem E, Sattath S, Kashtan N, Itzkovitz S, Milo R, Pinter RY, Alon U, Margalit H (2004) Network motifs in integrated cellular networks of transcription regulation and protein-protein interaction. *Proc Natl Acad Sci USA* **101:** 5934–5939

Zhang L, Hu G, Cheng Y, Huang J (2008) Heterotrimeric G protein α and β subunits antagonistically modulate stomatal density in *Arabidopsis thaliana*. *Dev Biol* **324:** 68–75

Zimmermann IM, Heim MA, Weisshaar B, Uhrig JF (2004) Comprehensive identification of *Arabidopsis thaliana* MYB transcription factors interacting with R/B-like BHLH proteins. *Plant J* **40:** 22–34